Optical and Quantum Electronics (2023) 55:796
https://doi.org/10.1007/s11082-023-05074-3

Manipulation speed of light and giant phase shifting: a new quantum-based model for improving efficiency and security of internet of things

Fazal Karim[1] · Muhammad Haneef[1] · Syed Sajid Ullah[2] · Majed Alsafyani[3] · Roobaea Alroobaea[3] · Sultan Algarni[4] · Saddam Hussain[5]

Received: 19 April 2023 / Accepted: 11 June 2023 / Published online: 30 June 2023

Abstract
The Internet of Things (IoT) is transitioning towards Quantum Computing soon, relying on electromagnetic waves for data transfer within circuits and between IoT devices. This paper introduces a four-level atomic medium controlled by electromagnetic fields to manipulate the speed of light, resulting in subluminal and superluminal information transfer for IoT. Subluminal propagation transmits data at an average rate, while superluminal propagation transfers data faster than conventional methods. The differentiation between these two modes of propagation is determined by the sign of the group index, which is positive for subluminal and negative for superluminal. Our proposed model reports a maximum positive and negative group index of ± 5000. This modified group velocity to become $v_g = \pm c/5000$ enhances IoT information transferring in quantum-based communication. The group delay time is measured to $t_d = \pm 10\mu s$ in the medium, which increases the capacity for IoT information storage. The maximum value of normal and anomalous phase shift is reported to $\Phi = \pm 20000$ radians at $60cm$ lengths of the medium; this effect is used to divide information in sub-set that protect IoT information from different types of attacks and losses.

Keywords Quantum communication · Superluminal propagation · Subluminal propagation · Cloaking

1 Introduction

Recently, the world has continuously passed through technological innovation concerning to Internet of Things (IoT) (Schöffel et al. 2022). Current improvement in the field of IoT aims to enhance speed, efficiency, storage capacity, and security through quantum techniques (Guatam et al. 2022). The based quantum techniques and communications use electromagnetic waves (light) as a medium within the circuit and signal processing for IoT devices (Arif et al. 2022). The fast invention of quantum-based IoT communication and devices demands an advanced quantum model that effectively controls and manages light speed (Larasati et al. 2021; Liu et al. 2022; Suriya 2022).

Extended author information available on the last page of the article

Normally, electromagnetic fields are used to manipulate the speed of light (Bhatt and Sharma 2019). In a medium, the electric susceptibility is investigated to control the group index and further the group velocity of light (Southall et al. 1816). The group index is either positive or negative. The positive value corresponds to the normal dispersion and the negative to the anomalous dispersion. The positive group index is related to slow group velocity (subluminal propagation) and the negative group index is related to faster than vacuum speed c of group velocity (superluminal propagation). In superluminal propagation, information transfers faster than conventional speed, enhancing the efficiency of IoT device circuits. The quantum-based IoT devices' circuits and signal processing are directly related to superluminal propagation (Kitano et al. 2003). The more superluminal boosting the speed of quantum-based devices.

Another main concern is to enhance the storage capacity of tiny IoT devices and chips. A quantum effect of delay time is used for this purpose. The delay time is the difference between times in a medium and free space (Arif et al. 2021a). The group delay time is related to the group pulse index in the medium. The delay time has two possible values i.e.: positive and negative. The positive delay time deals with normal storage capacity, while its negative value corresponds to increase storage capacity.

The transfer of IoT information over traditional security techniques is associated with security risks (Fernández-Caramés 2020). Researchers are considering reconnoitring quantum security techniques for wired IoT networks and circuits. One of its main advantages is that it can significantly increase the security and reliability of data transfer (Fernández-Caramés 2020). Also, quantum security can provide complete security and is suitable for long-distance IoT communication. Therefore, the solution incorporates quantum physics (Cheng et al. 2017; Fernández-Caramés et al. 2016). But still, the quantum state will be affected if the eavesdropper attempts to attack, measure, or duplicate anything in quantum-based communication (Sharma and Banerjee 2018). In quantum-based communications, eavesdropping refers to the unauthorized interception of quantum-based IoT information transmitted between two parties (Sharma 2016). An eavesdropper can intercept the quantum states exchanged between users or IoT devices to gain knowledge about the secret key without being detected. Phase shifting is an advanced technique that is used for IoT security enhancement in quantum physics. This technique divides the information packets into two parts, and the phase difference between them is measured. Based on this shift, cloaking devices are made that prevent IoT information from mentioned quantum attacks.

1.1 Motivation and contributions

Motivated by the above, we cover all the mentioned topics in this paper. The following are the main contributions of this paper.

- We used a four levels atomic medium driving by controlled electromagnetic fields to manipulate the speed of light.
- Our proposed model reports a maximum positive and negative group index of ± 5000.
- We modified the group velocity to become $v_g = \pm c/5000$, which enhances IoT information transferring in quantum-based communication.
- Subluminal and superluminal propagation are reported.

- We measured the group delay time to $t_d = \pm 10\mu s$ in the medium, increasing the capacity for IoT information storage.
- We achieved the normal and anomalous phase shift value to $\Phi = \pm 20{,}000$ rad at 60 cm length of the medium, protecting IoT information from different types of attack and losses.

1.2 Paper organization

The rest of this paper is structured as follows: Sect. 2 outlines the proposed network design and methodology, Sect. 3 presents and analyzes the results of our study, and Sect. 4 presents the deployment of our schemes in IoT. Finally, Sect. 5 provides a conclusion and summarization of our findings.

2 Models and methods

In this section, we provide IoT and atomic models for quantum-based communications.

2.1 Proposed quantum-based model for ioT devices and circuit

Quantum-based IoT devices Our model has two IoT devices: sender and receiver.

I.Sender side ioT device: The sender-side IoT devices are designed to transmit information using our designed quantum techniques. These techniques enable the secure and efficient transfer of information, which is critical to the system's functioning.

II.Receiver-side IoT device: The receiver-side IoT devices are designed to receive the information transmitted through our quantum technique. They play a crucial role in the overall system, as they are responsible for processing and receiving the quantum information transmitted by the sender IoT devices.

Quantum-based IoT circuits According to our established quantum technique, IoT circuits are designed to process and understand quantum information. They are essential to the overall operation of the system, as they are responsible for processing the quantum information received by the IoT receiver devices. These circuits process and transmit quantum information efficiently, ensuring the system's proper operation.

Quantum controller The Quantum Controller is a trusted third party responsible for controlling and regulating all quantum-based communications. It acts as a gatekeeper, ensuring only authorized parties can access the quantum-based communications network. This is achieved through our established security plan, which serves as a barrier against any potential outside hacking attempts. Ensuring the system's security and protecting the transmitted quantum information from unauthorized access or interference is vital (Fig. 1).

2.2 Proposed atomic system

A four-level atomic configuration is under consideration for the proposed aim and objective of IoT, as shown in Fig. 2. An electric probe fields E_p is driving between states 1 and 4. The Rabi frequency of this probe is Ω_p and detuning is Δ_p. A control field E_1 is driving between states 1 and 3. The Rabi frequency of the field is Ω_1 while detuning is Δ_1. Another

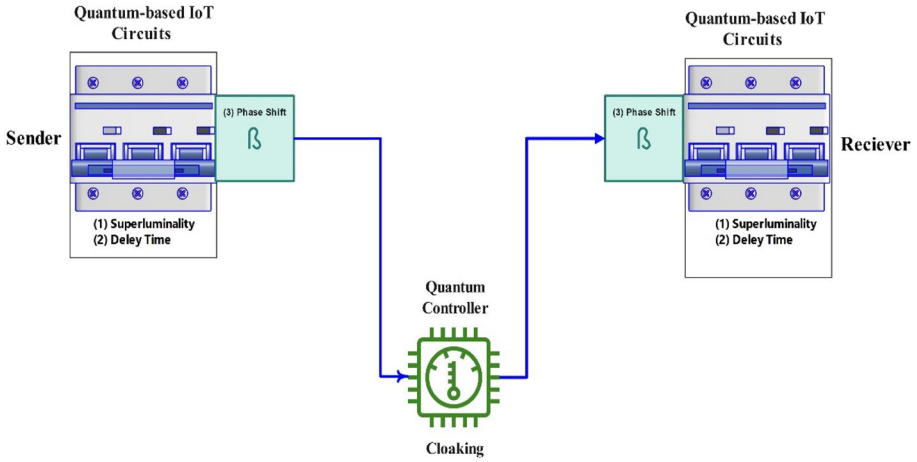

Fig. 1 Proposed Quantum-based Model for IoT Devices and Circuit

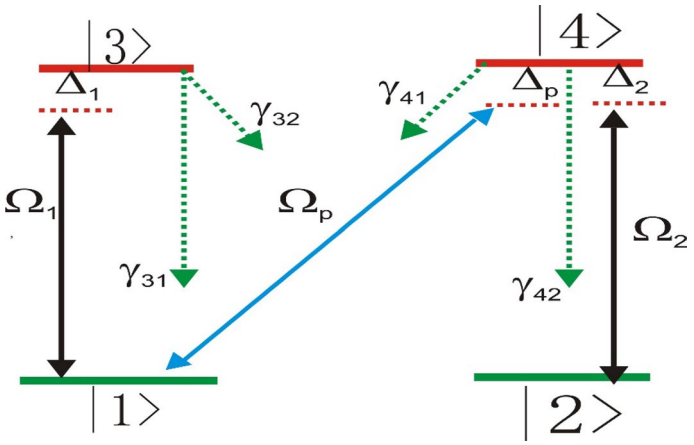

Fig. 2 Representation of a four-level atomic system

control field E_2 is driving between states 2 and 4. The Rabi frequency of the field is Ω_2 and detuning Δ_2. Both the control fields $E_{1,2}$ are responsible for the change in the atomic medium during the probe field E_p It is used to investigate those changes as well as the properties of the medium.

To treat the proposed atomic system quantum mechanically, an operator is applied. Here, the energy operator "Hamiltonian" is used. The Hamiltonian in the interaction picture describe the properties of the proposed system when external fields are applied and is given as (Arif et al. 2021b):

$$H = \quad - \frac{h}{2}[\Omega_p e^{-i\Delta_p t}|1\rangle\langle 4| + \Omega_1 e^{-i\Delta_1 t}|1\rangle\langle 3| + \Omega_2 e^{-i\Delta_2 t}|2\rangle\langle 4| + H.c. \tag{1}$$

The detuning of these fields is related to their corresponding angular frequencies and atomic states resonance frequencies as: $\Delta_p = \omega_{14} - \omega_1$, $\Delta_1 = \omega_{13} - \omega_1$, $\Delta_2 = \omega_{24} - \omega_2$.

Here, $\omega_{1,2}$ are the angular frequencies in states $|1\rangle$ and $|2\rangle$ while $\omega_{14,13,24}$ are the atomic states resonance frequencies between states $|1,4\rangle, |1,3\rangle$ and $|2,4\rangle$ respectively. A full-scaled density matrix calculation is performed to modify optical responses' coherence and electric susceptibility. To find the elements of the density matrix ρ, the following Lindblad master equation is used (Arif et al. 2021c).

$$\dot{\rho} = -\frac{\iota}{h}\left[\rho, H_I\right] = \frac{1}{2}\sum \gamma_{ij}\left(\alpha^{\dagger}\alpha\rho + \rho\alpha^{\dagger}\alpha - 2\alpha\rho\alpha^{\dagger}\right) \tag{2}$$

where $\alpha^{\dagger}$ is raising operator, and α is lowering operators while γ_{ij} Indicate the decay rates of various atomic states. Each element of the density matrix is represented by ρ. After explicitly time-independent simplification, the following coupled rates equations are obtained.

$$\dot{\tilde{\rho}}_{14} = A_1\tilde{\rho}_{14} + \frac{i}{2}\Omega_1\tilde{\rho}_{34} - \frac{i}{2}\Omega_2\tilde{\rho}_{12} + \frac{i}{2}\Omega_p\left(_{44} - \tilde{\rho}_{11}\right) \tag{3}$$

$$\dot{\tilde{\rho}}_{12} = A_2\tilde{\rho}_{12} + \frac{i}{2}\Omega_1\tilde{\rho}_{32} - \frac{i}{2}\Omega_2\tilde{\rho}_{14} + \frac{i}{2}\Omega_p\tilde{\rho}_{42} \tag{4}$$

$$\dot{\tilde{\rho}}_{32} = A_3\tilde{\rho}_{32} + \frac{i}{2}\Omega_1\tilde{\rho}_{12} - \frac{i}{2}\Omega_2\tilde{\rho}_{34} \tag{5}$$

$$\dot{\tilde{\rho}}_{34} = A_4\tilde{\rho}_{34} + \frac{i}{2}\Omega_1\tilde{\rho}_{14} - \frac{i}{2}\Omega_2\tilde{\rho}_{32} + \frac{i}{2}\Omega_p\tilde{\rho}_{31} \tag{6}$$

In all these equations, $\tilde{\tilde{\rho}}_{ij}$ are the coherence terms that represent the superposition (coupling) of states i and j in terms of the Rabi frequencies $\Omega_{p,1,2}$ of probe and control fields, the spontaneous decay γ_{ij} as well as detunings of the fields $\Delta_{1,2,p}$. These equations indicate the influence of one state upon another when taken collectively (mixed states). Further, A_1, A_2, A_3 and A_4 are given below:

$$\begin{aligned}
A_1 &= i\Delta_p - \frac{1}{2}\left(\gamma_{41} + \gamma_{31}\right)\\
A_2 &= i(\Delta_p - \Delta_2) - \frac{1}{2}\left(\gamma_{41} + \gamma_{31} + \gamma_{32} + \gamma_{42}\right)\\
A_3 &= i(\Delta_p - \Delta_2 - \Delta_1) - \frac{1}{2}\left(\gamma_{32} + \gamma_{42}\right)\\
A_4 &= i\left(\Delta_p - \Delta_1\right)
\end{aligned}$$

Applying the first-order perturbation condition to the coupled rates equations while taking Ω_1 in the first order and $\Omega_{1,2}$ in all orders. The atoms are prepared in the ground state $|1\rangle$. The population in the other states are assumed to be zero. This implies that its density element $\rho^{(0)} = 1$. Then the population in other states are zero, such as $\rho^{(0)}_{22,33,44} = 0$. Applying first-order perturbation condition, the coupled density matrix equation has solved by the following integral (Khan et al. 2020)

$$W(t) = \int_{-\infty}^{t} e^{-Y(t-t')}Qdt = Y^{-1}Q. \tag{7}$$

where $W(t)$ and Q are column matrices, and Y is a 3 by 3 matrix to solve coupled equations of $\rho_{14,12,13}$. The solution for first-order probe coherence is the following.

$$\tilde{\rho}_{14}^{(1)} = \frac{-2i\left(4A_2A_3A_4 + A_4\left|\Omega_1\right|^2\right)}{\left|\Omega_1\right|^4 + 2\left|\Omega_1\right|^2\left(2A_2A_3 + 2A_1A_4 - \left|\Omega_2\right|^2\right) + \left(4A_1A_2 + \left|\Omega_2\right|^2\right)\left(4A_4A_3 + \left|\Omega_2\right|^2\right)} \tag{8}$$

The electric coherence term $\tilde{\rho}_{14}^{(1)}$ is related to electric polarization as

$$P = N\sigma_{14}\tilde{\rho}_{14}^{(1)}, \tag{9}$$

where "σ_{14}" The dipole matrix element is calculated from Einstein coefficients as $\sigma_{14} = \sqrt{\frac{3\pi h\gamma_{14}\varepsilon_o c^3}{\omega^3}}$. The electric polarization in terms of electric susceptibility is, in the available literature:

$$P = \varepsilon_o\chi_e E \tag{10}$$

To find out about the dispersion and absorption, the electric susceptibility is calculated by comparing Eq. (8) and Eq. (10), as

$$\chi_e = \frac{N\sigma_{14}^2\rho_{14}}{\varepsilon_o h\Omega_p}. \tag{11}$$

The group index is written by

$$n_g = 1 + 2\pi Re\left(\chi_e\right) + 2\pi\omega\frac{\partial Re\left(\chi_e\right)}{\partial\Delta_p}. \tag{12}$$

where $D = \frac{\partial Re\left(\chi_e\right)}{\partial\Delta_p}$ is the dispersion term of the given medium.

To enhance the storage capacity of IoT devices, the "group delay time" is measured by the following relation.

$$t_d = \frac{L}{c}\left(n_g - 1\right). \tag{13}$$

The divide the IoT information in subsets, the "phase shifts" is calculated through the following equation:

$$\Phi = kL. \tag{14}$$

where $k = k_o n_r$ and L is the length of the medium. Furthermore, $n_r = 1 + 2\pi Re\left(\chi_e\right)$, while $k_o = {}^{2\pi}/_{\lambda} = {}^{\omega}/_{c}$.

3 Results and discussion

The graphical results are presented for subluminal and superluminal propagation and giant phase shifting through atomic medium to address the fourth-mentioned issues of IoT devices and communication. The decay rate for the system is supposed as $\gamma = 2\pi \times 10^9 Hz$. The other decays between two states, the Rabi frequencies, the detuning

of the fields, and angular frequency are scaled to this decay rate γ. $h = 2\pi(1.05) \times 10^{-34} Js$, $\varepsilon_o = 8.85 \times 10^{-12} F/C$, $\lambda = 2\pi c/\omega$, $\omega = 1000\gamma$ and the speed of light in vacuum is $c = 3 \times 10^8 m/s$. Further, $\gamma_{41,42,31,32} = 1\gamma$ and $L = 0.6cm$.

The results and discussion are explained with graphs in the following paragraph.

In Fig. 3, the plots are traced for the imaginary part of susceptibility versus Δ_p/γ, $|\Omega_{1,2}|/\gamma$, and $\Delta_{1,2}/\gamma$. The imaginary part of susceptibility is related to the absorption spectrum of the medium. The absorption is a robust oscillating function of probe detuning Δ_p/γ and control fields Rabi frequencies $\Omega_{1,2}/\gamma$. We check the absorption in the medium under different control parameters. The absorption is maximum in the resonance point $\Delta_p = 0$ at low Rabi frequencies $\Omega_{1,2} < 3\gamma$. As the Rabi frequencies are increased $\Omega_{1,2} > 3\gamma$, the single absorption peak is split into triplets. One peak is at the resonance point $\Delta_p = 0$ and the other two are in the positive and negative detuning regions. The peak is shifted toward the higher value of positive and negative detuning as the value of Rabi frequencies of control fields increases, as shown in Fig. 3a. The three absorption peaks are clearly reported with probe detuning slowly fluctuating with the phase of control fields Rabi frequencies. The complex Rabi frequencies are written as $\Omega_1 = \Omega_1 \exp(i\varphi_1)$ and $\Omega_2 = \Omega_2 \exp(i\varphi_2)$ as shown in Fig. 3b. The absorption is a robust oscillating function of control fields detuning $\Delta_{1,2}/\gamma$. The absorption is minimized at the control field E_1 of resonance point $\Delta_1 = 0$ and minimizes at the control field E_2 of resonance point $\Delta_2 = 0$, as shown in Fig. 3c. From the behavior of the graph, it is clear that the absorption of the probe field can be controlled by changing detuning, and the losses in the medium can be minimized, enhancing the system's efficiency.

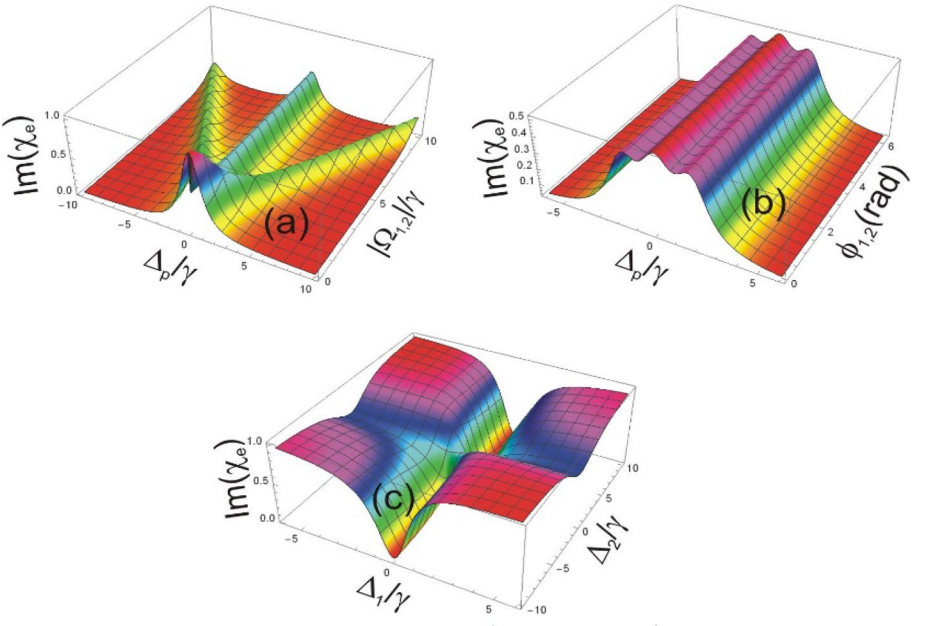

Fig. 3 **a** imaginary part of susceptibility versus Δ_p/γ and $|\Omega_{1,2}|/\gamma$ such as $\Delta_{1,2} = 0$, $\varphi_1 = \pi/3$, $\varphi_2 = \pi/4$ **b** the imaginary part of susceptibility versus Δ_p/γ and $\varphi_{1,2}$ such as $\Delta_{1,2} = 0$, $|\Omega_{1,2}| = 2\gamma$ **c** imaginary part of susceptibility versus $\Delta_{1,2}/\gamma$ such as $\Delta_p = 0$, $|\Omega_{1,2}| = 2\gamma$, $\varphi_{1,2} = \pi/4$

In Fig. 4, the plots are traced for the real part of susceptibility versus Δ_p/γ, $|\Omega_{1,2}|/\gamma$, and $\Delta_{1,2}/\gamma$. The real part of susceptibility is related to the dispersion spectrum of the medium. The dispersion is also a robust oscillating function of probe detuning Δ_p/γ and control fields Rabi frequencies $\Omega_{1,2}/\gamma$. The positive slope of dispersion $\partial(Re(\chi)/\partial\Delta p > 0$ shows normal dispersion, and the negative slope of dispersion $\partial(Re(\chi)/\partial\Delta p < 0$ is called anomalous dispersion. The dispersion is anomalous at resonance point $\Delta p = 0\gamma$ at low Rabi frequencies $\Omega_{1,2} < 3\gamma$.. As the Rabi frequencies $\Omega_{1,2} > 3\gamma$, the single absorption peak is split into triplets. The dispersion at the triplet absorption peaks region is anomalous. When absorption increases, the slope becomes anomalous, and when absorption decreases, the dispersion slope becomes normal. At the resonance point $\Delta_p = 0$ of absorption peak region, the dispersion slope is anomalous, and the other two peaks occur at positive and negative detuning regions; the slope of dispersion is again anomalous. The anomalous dispersion regions are shifted toward the higher value of positive and negative probe detuning as the value of Rabi frequencies of control fields increases, as shown in In Fig. 4a. The slope is anomalous at the three absorption peaks region and slowly fluctuation with the phase of control fields $\varphi_{1,2}$ as shown In Fig. 4b. The dispersion is normal at the control field E_1 of resonance point $\Delta_1 = 0$ and normal at the control field E_2 of resonance point $\Delta_2 = 0$, as shown in In Fig. 4c.

In superluminal propagation, information transfers faster than conventional speed, enhancing the efficiency of IoT devices and quantum circuits. The quantum-based IoT devices' circuits (Vishal et al. 2021; Sharma and Banerjee 2020) and signal processing are directly related to superluminal propagation. The more superluminal boosting the speed of quantum-based devices. In Fig. 5, the plots are traced for group index versus Δ_p/γ, $\Omega_{1,2} = \gamma$, $\varphi_{1,2}$ and $\Delta_{1,2}/\gamma$. The group index is related to the group velocity of the pulse in

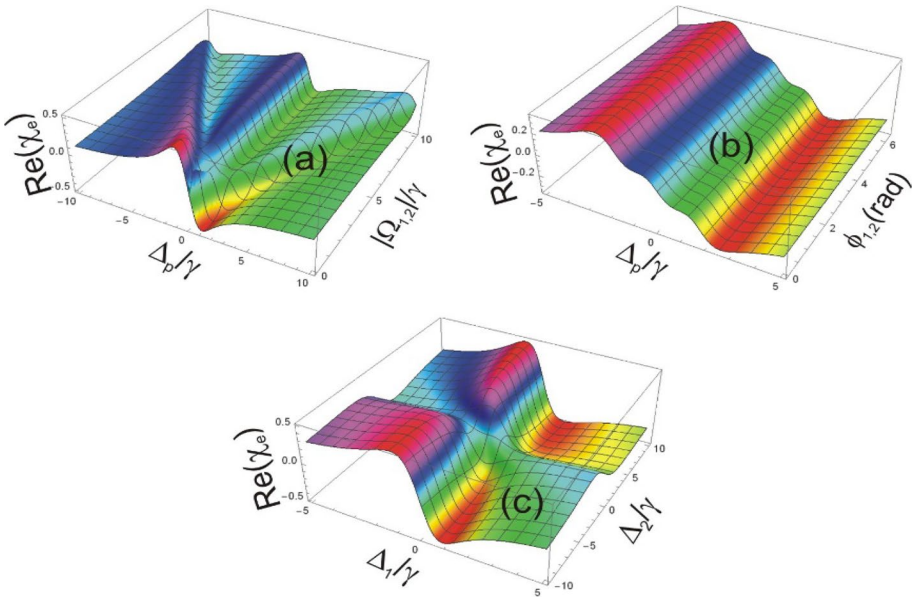

Fig. 4 **a** Real part of susceptibility versus Δ_p/γ and $|\Omega_{1,2}|/\gamma$ such as $\Delta_{1,2} = 0$, $\varphi_1 = \pi/3$, $\varphi_2 = \pi/4$ **b** Real part of susceptibility versus Δ_p/γ and $\varphi_{1,2}$ such as $\Delta_{1,2} = 0$, $|\Omega_{1,2}| = 2\gamma$ **c** Real part of susceptibility versus $\Delta_{1,2}/\gamma$ such as $\Delta_p = 0$, $|\Omega_{1,2}| = 2\gamma$, $\varphi_{1,2} = \pi/4$

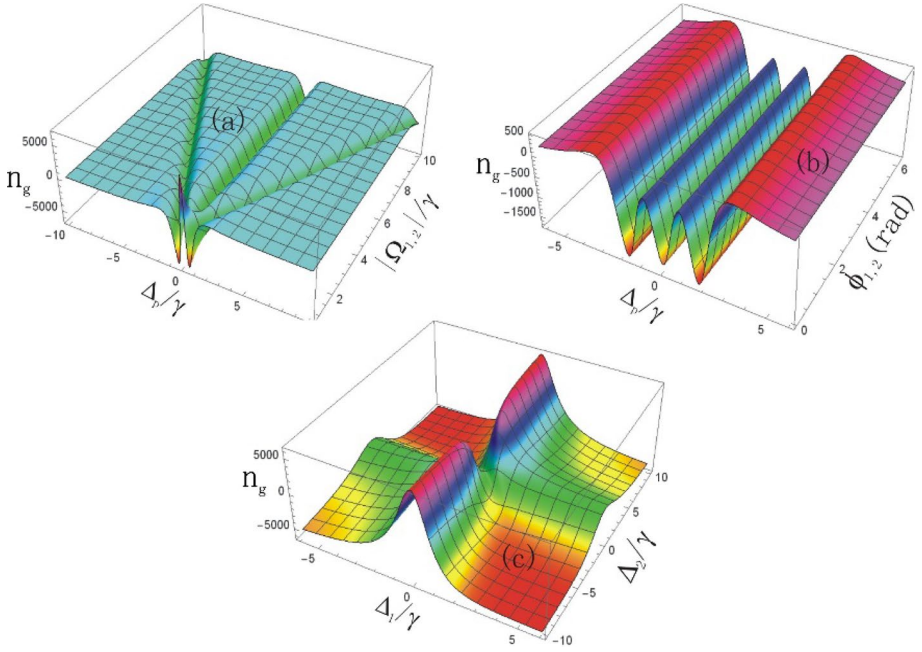

Fig. 5 **a** Group index versus Δ_p/γ and (|Ω_1,2|)/γ such as Δ_1,2 = 0, φ_1 = π/3, φ_2 = π/4 **b** Group index versus Δ_p/γ and φ_1,2 such as Δ_1,2 = 0, |Ω_1,2| = 2γ **c** Group index versus Δ_1,2/γ such as Δ_p = 0, |Ω_1,2| = 2γ, φ_1,2 = π/4.

the medium as $v_g = c/n_g$. The group index is also a strong oscillating function of probe detuning Δp/γ and control fields Rabi frequencies $\Omega_{1,2} = \gamma$. The group index is positive in the normal dispersion region and negative in the anomalous dispersion region. The positive group index is related to slow group velocity (subluminal propagation), and the negative group index is related to faster than vacuum speed c of group velocity (superluminal propagation). A large negative group index of 5000 is reported in the anomalous dispersion region at large absorption peak regions. At this region, the group velocity becomes $v_g = c/5000$. This shows superluminal propagation because negative group velocity is faster than vacuum speed c, as shown in Fig. 5a. The superluminal effect is used to enhance the efficiency of circuits in IoT devices. This effect is also used to increase the information-transferring speed in quantum-based communication. The group index is also a function of the probe detuning and phases of control fields φ1,2. In this case, the group index is negative in the anomalous dispersive region and has a maximum negative value of 1500, which corresponds to a negative group velocity of $v_g = c/1500$. The group index slowly varies with phases $\varphi_{1,2}$ as shown in Fig. 5b. The group index is positive, having a value of 5000 at the control field E_1 of resonance point $\Delta_1 = 0$, and the control field E_2 of resonance point $\Delta_2 = 0$. In this case, the group velocity has a positive value $v_g = c/5000$. The slow group velocity $v_g << c$, and called subluminal propagation of light pulse as shown in Fig. 5c.

A quantum effect of delay time is used to enhance the storage capacity of tiny IoT devices and chips. The delay time is the difference between medium and free space times. The delay time has two possible values, i.e., positive, and negative. The positive delay time deals with normal storage capacity, while its negative value corresponds to increase storage capacity. In Fig. 6, the plots are traced for group delay time versus Δ_p/γ,

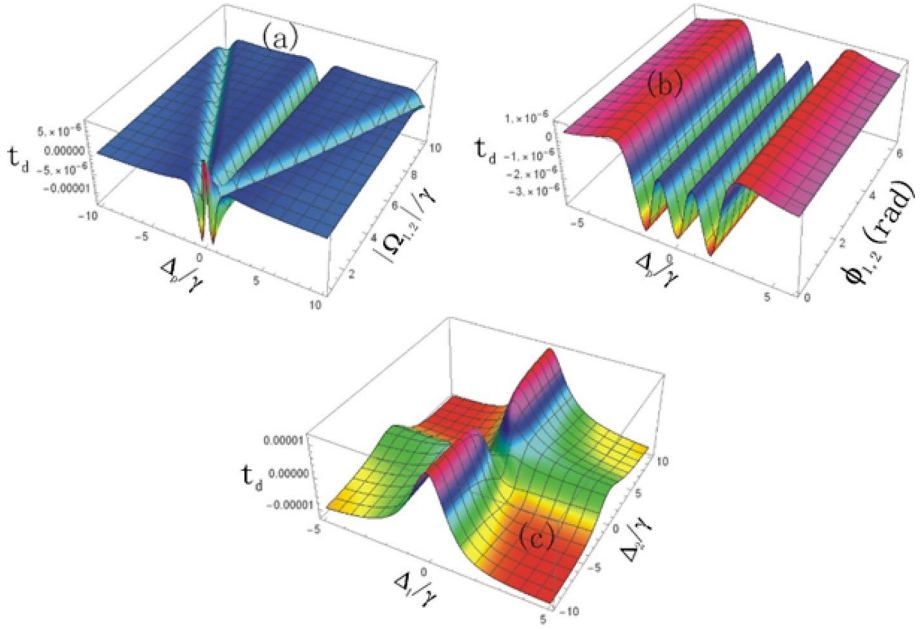

Fig. 6 **a** Group delay time versus Δ_p/γ and (|Ω_1,2 |)/γ such as Δ_1,2 = 0, φ_1 = π/3, φ_2 = π/4 **b** Group delay time versus Δ_p/γ and φ_1,2 such as Δ_1,2 = 0, |Ω_1,2| = 2γ **c** Group delay time versus Δ_1,2/γ such as Δ_p = 0, |Ω_1,2| = 2γ, φ_1,2 = π/4.

$\Omega_{1,2}/\gamma$, $\varphi_{1,2}$ and $\Delta_{1,2}/\gamma$. The negative value of delay time is used to increase the storage capacity of IoT devices. Further, it gives rise to the superluminal effect, which is responsible for increasing the efficiency of IoT devices. The delay time is related to the group index of pulse in the medium in relation $t_d = t_m - t_v = \mathrm{L}(n_g - 1)/\mathrm{c}$. Where $t_v = \mathrm{L}/\mathrm{c}$ and $t_m = \mathrm{L}/v_g$. If t_d is positive, then $t_m > t_v$ and this is true for the positive value of n_g. If t_d is negative, then $t_m < t_v$ and this is true for the negative value of n_g. But for a negative value of n_g, both t_d and v_g are negative. So, at negative group velocity, the time of the pulse in the medium is shorter than the time of the pulse in the vacuum $t_m < t_v$ at the same length, L. Therefore, the negative group velocity is faster than c because $t_m < t_v$. The group delay time is a strong function of probe detuning Δ_p/γ and control fields Rabi frequencies $\Omega_{1,2}/\gamma$. A large negative group delay time is reported in the negative group index regions that occur at the absorption peak region of anomalous dispersions. The value of group delay time in these regions is $t_d = 10\mu s$, which shows superluminal propagation as shown in Fig. 6a. The group delay is also a function of probe detuning Δ_p/γ and phases of control fields $\varphi_{1,2}$. In this case, the group delay is investigated to $H = -\frac{h}{2}[\Omega_p e^{-i\Delta_p t}|1\rangle\langle 4| + \Omega_1 e^{-i\Delta_1 t}|1\rangle\langle 3| + \Omega_2 e^{-i\Delta_2 t}|2\rangle\langle 4| + H.c.$ in large anomalous dispersive regions, which is a superluminal effect as shown in Fig. 6b. The group delay time is also a function of control field detuning's $\Delta_{1,2}/\gamma$. The maximum value of delay time with probe detuning is $t_d = 10\mu s$. At the resonance point of control field E_1 of $\Delta_1 = 0$, the delay time has a positive value of $t_d = 10\mu s$, which indicates the subluminal propagation of light pulse in the medium, as shown in Fig. 6c.

Phase shifting is used for IoT security enhancement in quantum physics (Sharma and Bhardwaj 2022). This technique divides the information packets into two parts, and the phase

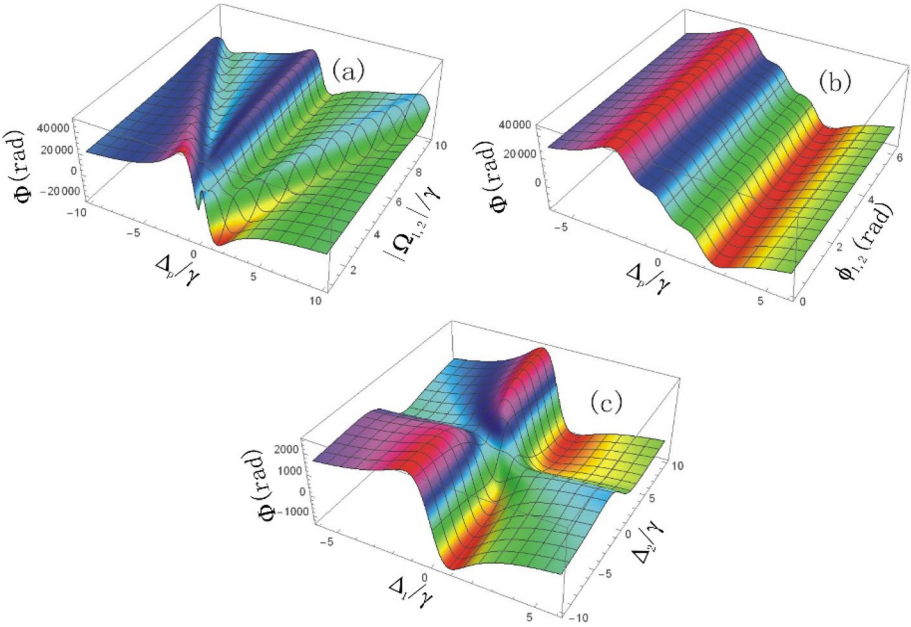

Fig. 7 **a** Phase shift versus Δ_p/γ and (|Ω_1,2|)/γ such as Δ_1,2 = 0, φ_1 = π/3, φ_2 = π/4 **b** Phase shift versus Δ_p/γ and φ_1,2 such as Δ_1,2 = 0, |Ω_1,2| = 2γ **c** Phase shift versus Δ_1,2/γ such as Δ_p = 0, |Ω_1,2| = 2γ, φ_1,2 = π/4.

difference between them is measured. Based on this shift, cloaking devices are made that prevent IoT information from attacks. In Fig. 7, the plots are traced for the phase of the pulse through the 60 cm length of the medium versus Δ_p/γ, $\Omega_{1,2}/\gamma$, $\varphi_{1,2}$ and $\Delta_{1,2}/\gamma$. When two information-carrying EM beams enter the atomic medium, a phase shift is generated by adjusting the medium's control field frequencies, detunings, and spinning. Now, the two beams are not present at the same point, at the same time domain; hence, the IoT information is divided into subsets, making it difficult for hackers to trace and detect it. Further, suppose the two beams entering the medium destructively interfere. In that case, the energy losses occur, but as a result of the phase shift, the beams are separated through an angle which not only prevents it from interference but also does not change the frequency or amplitude and hence no energy losses occurs. The phase shift is related to dispersion in the medium. Normal dispersion is related to normal phase shift, and anomalous is related to anomalous phase shift. Here, the phase shift is a strong function of probe detuning Δ_p/γ and control fields Rabi frequencies $\Omega_{1,2}/\gamma$. A giant anomalous phase shift reported in the negative group index regions occurs at the absorption peak region, where anomalous dispersions occur. The value of normal and anomalous phase shift in these regions is $\Phi = 2000$ radian at 60 cm length of the medium, as shown in Fig. 7a. The phase is also a function of probe detuning Δ_p/γ and phases of control fields $\varphi_{1,2}$. In this case, the giant phase shift of 4000 radians to 1500 radians is investigated with a variation of Δ_p/γ and $\varphi_{1,2}$ as shown in Fig. 7b, the phase shift is also a function of control fields detunings $\Delta_{1,2}/\gamma$. The maximum value of phase shift is investigated with a variation of the control fields detuning $\Delta_{1,2}/\gamma$ to ± 1500, as shown in Fig. 7c. This large value indicates the better efficiency of the proposed scheme.

4 Deployment and workflow process in IoT

In this section, we provided the deployment of our scheme in quantum-based IoT devices. We divided deployment into the following three sub-parts.

4.1 Enhancing speed of data/information processing in quantum-based IoT

We investigated the negative and positive group indexes. The positive value corresponds to the normal and the negative to the anomalous dispersion. The positive group index is related to slow group velocity (subluminal propagation), and the negative group index is related to faster than vacuum speed c of group velocity (superluminal propagation). In superluminal propagation, information transfers faster than conventional speed, enhancing the efficiency of IoT device circuits. Quantum-based IoT devices and signal processing are directly related to superluminal propagation. The more superluminal boosting the speed of quantum-based devices. As shown in Fig. 8.

4.2 Enhancing storage capacity for quantum-based IoT

We also investigated the delay time enhancing storage capacity for quantum-based IoT devices. The delay time is the difference between medium and free space times, and the group delay time is related to the group pulse index in the medium. The delay time has two possible values, i.e., positive and negative. The positive delay time deals with normal storage capacity, while its negative value corresponds to increase storage capacity, as shown in Fig. 9.

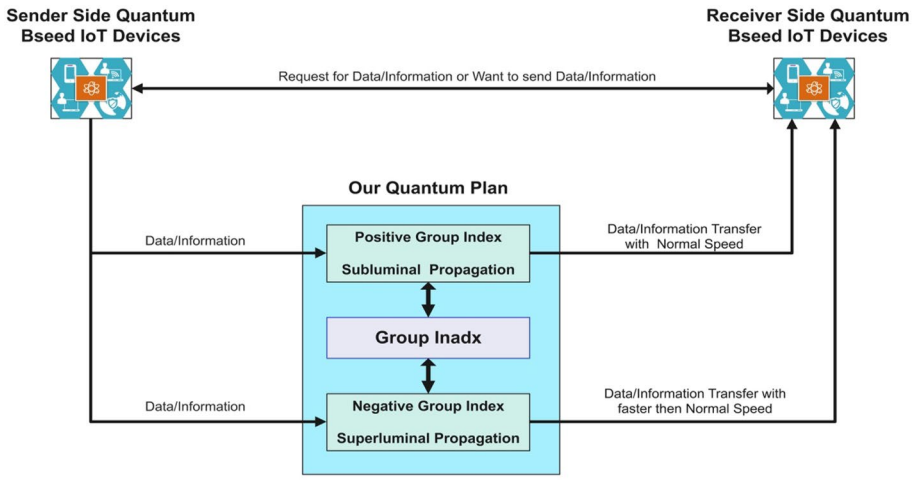

Fig. 8 Enhancing Speed of Quantum-based IoT Data/Information Processing in Subluminal and Superluminal Propagation

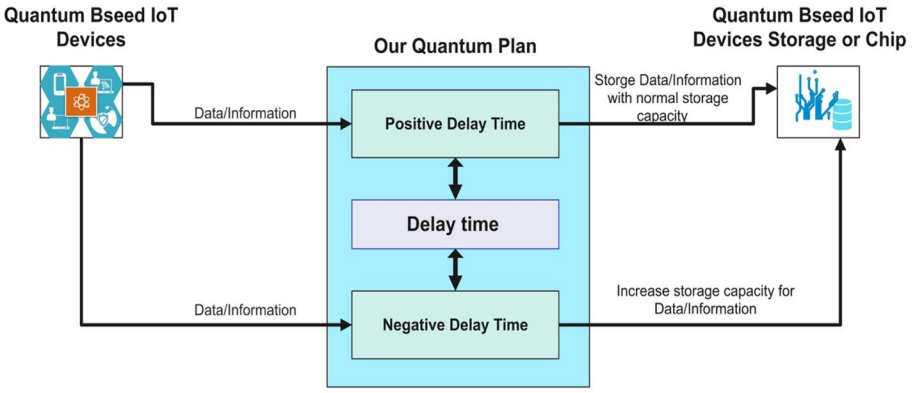

Fig. 9 Improving Storage Capacity for Quantum-based IoT

4.3 Enhancing security for quantum-based iot using phase shifting

In our scheme, Phase shifting is used for IoT security enhancement in Quantum-based IoT. This technique divides the information packets into two parts, measuring their phase difference. Based on this shift, cloaking devices prevent IoT information from attacks. The quantum state will be affected if the eavesdropper attempts to attack, measure, or duplicate anything in quantum communication. Therefore, it is unlikely that the recipient will be able to be distracted, as shown in Fig. 10.

In quantum cryptography, phase shifting is an essential building block contributing to information protection. Photons, the individual particles of light used in transmitting information in quantum key distribution protocols, are referred to as qubits. These photons can exist in various quantum states, translated into the ones and zeros that make up binary code. Before a photon can be transmitted, it must first have its quantum state phase-shifted

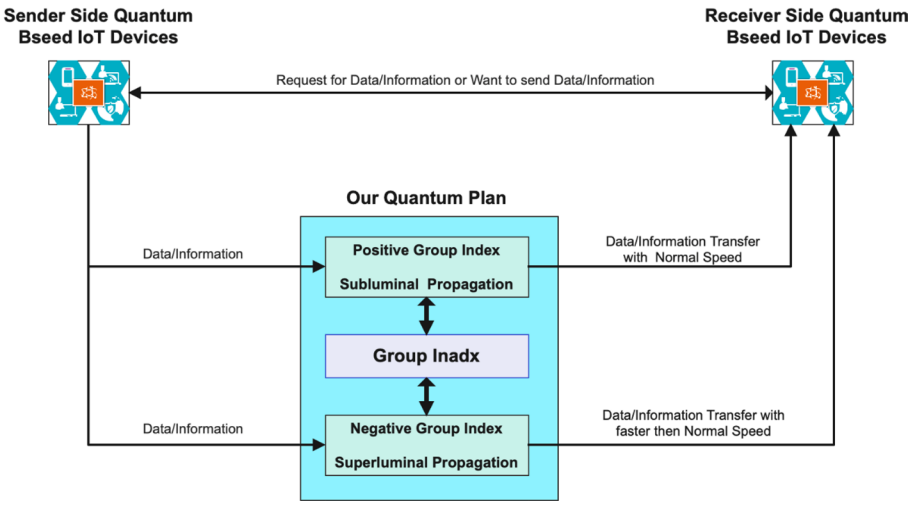

Fig. 10 Enhancing Security for Quantum-based IoT Using Phase Shifting

by adding a random amount of phase shift (Phase shifting). Any attempt to measure the photons would disturb the phase shift, thereby changing the state of the photon and making it impossible to interpret the original information, making it extremely difficult for an eavesdropper to intercept the transmission and obtain any helpful information.

In addition, any measurement in quantum cryptography alters the state of the photons. Any attempt by an eavesdropper to intercept a transmission will leave behind evidence of the interference caused by the eavesdropper, giving legitimate users fair warning of the intruder's presence. Finally, phase shifting is a method used in quantum cryptography to guarantee confidential data transmission.

5 Conclusions

In our proposed Quantum-based model for IoT, A four levels atomic medium deriving by controlled electromagnetic fields is used to modify subluminal and superluminal propagation of light pulse and giant phase shifting. Density matric formalism is used to derive electric susceptibility, group index, group velocity, group delay time, and phase shift of pulses in the medium. Normal and anomalous dispersion are reported at low and high absorption regions. The group index is positive in the normal dispersion region and negative in the anomalous dispersion region. The positive group index is related to slow group velocity (subluminal propagation), while the negative group index is related to faster than vacuum speed c of group velocity (superluminal propagation). Our proposed work reports a large negative group index of 5000 in the anomalous dispersion region, occurring in large absorption peak regions. This modified group velocity to become $v_g = -c/5000$. that enhances IoT information transferring in quantum-based communication. The group delay time is related to the group index of pulse in the medium in relation $t_d = t_m - t_v = \mathrm{L}\left(n_g - 1\right)/\mathrm{c}$. The group delay time is measured to $t_d = \pm 10\mu s$ in the medium, this increases the capacity for IoT information storage. The maximum value of normal and anomalous phase shift is reported to $\Phi = \pm 20000$ radian at $60cm$ length of the medium; this effect is used to divide information in a sub-set that protects IoT information from different types of attacks and losses. Our work's control and modified results are useful to enhance the storage capacity of tinny IoT devices, build more efficient cloaking devices, enhance the data transfer speed, and protect IoT information from being hacked.

Author contributions FK contributed to the study design and data analysis. MH assisted in preliminary data analysis. SSU* is responsible for the overall study design, data interpretation, and manuscript preparation. MA contributed to data interpretation and provided critical input on the manuscript. RA participated in data analysis and manuscript revision. SA provided valuable insights during the study. SH contributed to the study design and critically reviewed the manuscript for intellectual content. All authors read and approved the final manuscript.

Funding Open access funding provided by University of Agder. The researchers would like to acknowledge Deanship of Scientific Research, Taif University for funding this work.

Data availability The data is available with the corresponding author on a reasonable request.

Declarations

Competing interests The authors declare no competing interests.

Conflicts of interest The authors declare no conflict of interest.

Ethical approval Not applicable.

References

Arif, S.M., Bacha, B.A., Wahid, U., Haneef, M., Ullah, A.: Tunable subluminal to superluminal propagation via spatio-temporal solitons by application of Laguerre fields intensities. Phys. Lett. A **388**, 127041 (2021a)

Arif, S.M., Bacha, B.A., Wahid, U., Ullah, A., Haneef, M.: Tunnelling based birefringent phase sensitivity through dynamic chiral medium. Phys. Scr. **96**, 035106 (2021b)

Arif, S.M., Bacha, B.A., Wahid, U., Haneef, M., Ullah, A.: Tunable subluminal to superluminal propagation via spatio-temporal solitons by application of laguerre fields intensities. Phy. Lett. A **388**, 127041 (2021c)

Arif, S.M., Bacha, B.A., Ullah, S.S.: Tunable control of internet of things information hacking by application of the induced chiral atomic medium. Soft Comput. **26**, 10643–10650 (2022)

Bhatt, A.P., Sharma, A.: Quantum cryptography for internet of things security. J. Electr. Sci. Technol. **17**, 213–220 (2019)

Cheng, C., Lu, R., Petzoldt, A., Takagi, T.: Securing the Internet of Things in a quantum world. IEEE Commun. Mag. **55**, 116–120 (2017)

Fernández-Caramés, T.M., Fraga-Lamas, P., Suárez-Albela, M., Castedo, L.: Reverse engineering and security evaluation of commercial tags for RFID-based IoT applications. Sensors **17**, 28 (2016)

Fernández-Caramés, T. M. From pre-quantum to post-quantum IoT security: a survey on quantum-resistant cryptosystems for the internet of things, In *IEEE Int. Things J.*, *7*, 6457–6480, (**2020**).

Guatam, S., Solanki, S., Sharma, S.K., Chatzinotas, S., Ottersten, B.: Boosting quantum-based IoT gadgets via RF-enabled energy harvesting. Sensors **22**, 5385 (2022)

Khan, S., Muhammad, S., Bacha, B.A., Wahid, U.: Birefringent lateral goos-hnchen effect through chiral medium. Phys. Scr. **95**(9), 095102 (2020)

Kitano, M.; Nakanishi T.; Sugiyama, K. Negative group delay and superluminal propagation: an electronic circuit approach. *IEEE J. Select.Top. Quantum Electr.*, *9,* 43–51 (2003).

Larasati, H.T., Awaludin, A.M., Ji, J., Kim, H.: Quantum Circuit Design of Toom 3-Way Multiplication. App. Sci. **11**, 3752 (2021)

Liu, G., Han, J., Zhou, Y., Liu, T., Chen, J.: QSLT: a quantum-based lightweight transmission mechanism against eavesdropping for IoT networks. Wireless Comm. Mob. Comp. **2022**, 13 (2022)

Schöffel, M., Lauer, F., Rheinländer, C.C., Wehn, N.: Secure IoT in the Era of quantum computers—where are the bottlenecks? Sensors **22**(7), 2484 (2022)

Sharma, V.: Effect of Noise on Practical Quantum Communication Systems." Def. Sci. J. **66**(2), 186–192 (**2016**).

Sharma, V., Banerjee, S.: Quantum communication using code division multiple access network. Opt. Quant. Electron. **52**(8), 1–22 (2020)

Sharma, Vishal, and Subhashish Banerjee. Analysis of quantum key distribution-based satellite communication. In 2018 9thInternational Conference on Computing, Communication and Networking Technologies (ICCCNT), pp 1–5. IEEE, (2018).

Sharma, Vishal, and Asha Bhardwaj. Analysis of differential phase shift quantum key distribution using single-photon detectors. In 2022 International Conference on Numerical Simulation of Optoelectronic Devices (NUSOD), pp 17–18. IEEE, (2022).

Southall, J., Hodgson, D., Purdy, R., Beige, A.: Comparing hermitian and non-hermitian quantum electrodynamics. Symmetry **2022**, 14 (1816)

Suriya, M. Machine learning and quantum computing for 5G/6G communication networks—a survey. *3,* 197–203, (**2022**).

Sharma Vishal, Shantanu Gupta, Gaurav Mehta, and Bhupesh K. Lad.A diagnostics approach for additive manufacturing machine. IET Collab. Intell. Manuf. 3, (2), 184–192, (2021)

Authors and Affiliations

Fazal Karim[1] · Muhammad Haneef[1] · Syed Sajid Ullah[2] · Majed Alsafyani[3] · Roobaea Alroobaea[3] · Sultan Algarni[4] · Saddam Hussain[5]

✉ Syed Sajid Ullah
syed.s.ullah@uia.no

Fazal Karim
fazalkarim3268@gmail.com

Muhammad Haneef
hanifsaqi85@gmail.com

Majed Alsafyani
alsufyani@tu.edu.sa

Roobaea Alroobaea
r.robai@tu.edu.sa

Sultan Algarni
saalgarni@kau.edu.sa

Saddam Hussain
saddamicup1993@gmail.com

[1] Department of Physics, Hazara University Mansehra, Mansehra 21120, Pakistan

[2] Department of Information and Communication Technology, University of Agder (UiA), N-4898 Grimstad, Norway

[3] Department of Computer Science, College of Computers and Information Technology, Taif University, P. O. Box 11099, Taif 21944, Saudi Arabia

[4] Department of Information Systems, Faculty of Computing and Information Technology, King Abdulaziz University, Jeddah 21589, Saudi Arabia

[5] School of Digital Science, Universiti Brunei Darussalam, Jalan Tungku Link, Gadong BE1410, Brunei